

Enhanced dielectric tunability properties of $\text{Ba}(\text{Zr}_x\text{Ti}_{1-x})\text{O}_3$ thin films using seed layers on $\text{Pt}/\text{Ti}/\text{SiO}_2/\text{Si}$ substrates

Jiwei Zhai ^{a,*}, Cheng Gao ^a, Xi Yao ^a, Zhengkui Xu ^b, Haydn Chen ^b

^a Functional Materials Research Laboratory, Tongji University, Shanghai 200092, China

^b Department of Physics and Materials Science, City University of Hong Kong, Kowloon, Hong Kong

Available online 4 October 2007

Abstract

The compositionally graded and homogeneous $\text{Ba}(\text{Zr}_x\text{Ti}_{1-x})\text{O}_3$ (BZT) thin films were fabricated on LaNiO_3 (LNO) buffered $\text{Pt}/\text{Ti}/\text{SiO}_2/\text{Si}$ and $\text{Pt}/\text{Ti}/\text{SiO}_2/\text{Si}$ substrates by a sol–gel deposition method, respectively. These films crystallized into a single perovskite phase. The BZT thin films deposited on $\text{LaNiO}_3/\text{Pt}/\text{Ti}/\text{SiO}_2/\text{Si}$ substrates had a highly (1 0 0) preferred orientation and exhibited a preferred (1 1 0) orientation when the thin films were deposited on $\text{Pt}/\text{Ti}/\text{SiO}_2/\text{Si}$ substrates. The LNO and $\text{Ba}(\text{Zr}_{0.30}\text{Ti}_{0.70})$ served as seed layer on $\text{Pt}/\text{Ti}/\text{SiO}_2/\text{Si}$ substrates and analyze the relationship of seed layer, microstructure and dielectric behavior of the thin films. The compositionally graded thin films from BaTiO_3 to $\text{BaZr}_{0.35}\text{Ti}_{0.65}\text{O}_3$ were fabricated on LNO/ $\text{Pt}/\text{Ti}/\text{SiO}_2/\text{Si}$ substrates. The tunability behavior of compositionally graded films was analyzed in order to produce optimum effective dielectric properties. The dielectric constant of $\text{BaZr}_x\text{Ti}_{1-x}\text{O}_3$ compositionally graded thin films showed weak temperature dependence. This kind of thin films has a potential in a fabrication of a temperature stable tunable device.

© 2007 Elsevier Ltd and Techna Group S.r.l. All rights reserved.

Keywords: A. Sol–gel processes; A. Films; C. Dielectric properties; Microstructure

1. Introduction

The large electrical field dependent dielectric constant can be used for tunable microwave devices, such as phase shifters, tunable oscillators, tunable filters and varactors. In such devices, it is desirable to have a high dielectric tunability over a given electric field range, a low dielectric loss and high Q value. Commonly, the studies in this field are mainly focused on the $\text{Ba}_x\text{Sr}_{1-x}\text{TiO}_3$ (BST) system [1–4].

There are a large number of lead-free BaTiO_3 -based ceramics and thin films with different composition, some of which exhibit a relax behavior with characteristics related to the type of ionic substitutes and substitution rate [5–8]. Barium zirconium titanate $\text{Ba}(\text{Zr}_x\text{Ti}_{1-x})\text{O}_3$ (BZT) is obtained by substituting ions at the B site of the BaTiO_3 with Zr in compounds of the perovskite structure ABO_3 . Depending on the amount of zirconium (Zr) substitution in BaTiO_3 , it behaves as a ferroelectric or a relaxor [9]. It is reported that an increase in the Zr content induces a reduction in the thin films grain size

and dielectric constant, and maintains the leakage current low and stable [5,8].

In the last few years, BZT ceramics has been used as a dielectric material in multi-layer ceramic capacitors (MLCC) and is of considerable interest for use as a new ferroelectric material for the dynamic random access memory (DRAM) and the piezoelectric transducer [5,10,11] in the future and more currently in tunable microwave applications due to their high dielectric constant, relatively low dielectric loss, leakage current and their tunable dielectric properties [12,13]. However, their tunable dielectric properties and the relationships of the orientation and seed layer effect were rarely investigated.

In the present investigation, an improvement in dielectric properties was achieved by the insertion of seed layers between the BZT and bottom electrode. The LaNiO_3 (LNO) and $\text{Ba}(\text{Zr}_{0.30}\text{Ti}_{0.70})$ thin films were as seed layer on $\text{Pt}/\text{Ti}/\text{SiO}_2/\text{Si}$ substrates. The use of LNO seed layer provides bottom electrode and an excellent template facilitating the grain-on-grain growth so that highly oriented BZT thin films with much improved properties are realized. In order to improve temperature stability from the compositionally graded thin films along with improved tunability, the compositional gradient thin films from BaTiO_3 to $\text{BaZr}_{0.35}\text{Ti}_{0.65}\text{O}_3$ were

* Corresponding author. Tel.: +86 21 65980544; fax: +86 21 65985179.

E-mail address: apzhai@mail.tongji.edu.cn (J. Zhai).

fabricated on LNO/Pt/Ti/SiO₂/Si substrates. The relationship of seed layer, microstructure and dielectric behavior of the thin films were studied. The tunability behavior of graded films was analyzed in order to produce optimum effective dielectric properties.

2. Experimental procedure

The barium acetate [Ba(CH₃COO)₂] (99%, Sigma–Aldrich), [Zr(OC₃H₇)₄] (99.9% Aldrich), and [Ti(OC₃H₇)₄] (98%, Aldrich) were used as starting materials. Acetic acid was used as solvent. The details of the preparation of BZT solution have been described in our early publication [14]. The concentration of the final solution was adjusted to about 0.3 M. The LNO layer was deposited on platinumized Si substrates using the magnetron sputtering technique [15]. The thicknesses of the LaNiO₃ (LNO), Pt, Ti, and SiO₂ were 150, 150, 50, and 150 nm, respectively.

The seed layer of Ba(Zr_{0.30}Ti_{0.70}) was deposited on Pt/Ti/SiO₂/Si substrates by sol–gel processing. The concentration of the solution was adjusted to about 0.1 M. Pyrolysis and heat treatment were carried out in an air muffle furnace at 700 °C for 10 min for each spun-on coating. The different seed layer thickness was achieved by repeated spin coating–drying–annealing process. The different BZT seed layer thicknesses of 0, 10, 20, 30 and 90 nm were obtained, respectively.

After aging the hydrolyzed solution for 24 h, the homogeneous Ba(Zr_xTi_{1–x})O₃ (BZT) thin film was carried out on the LaNiO₃/Pt/Ti/SiO₂/Si(1 0 0) and Ba(Zr_{0.30}Ti_{0.70})/Pt/Ti/SiO₂/Si(1 0 0) substrates by spin coating at 3000 rpm for 30 s each layer, respectively. Each spin coated BZT layer was subsequently heat treated at 500 °C for 5 min. The coating and heat treatment procedures were repeated several times until the desired thickness was reached. A final anneal in flowing O₂ (decrease leakage current) at high temperature of 700 °C for 30 min crystallize the amorphous films. The total film thickness of BZT was about 480 nm.

Compositionally graded BaZr_xTi_{1–x}O₃ thin films were formed on the LNO/Pt/Ti/SiO₂/Si substrate by sequentially depositing three layers of each composition (sequence: BaZr_{0.35}Ti_{0.65}O₃, BaZr_{0.18}Ti_{0.82}O₃, BaZr_{0.09}Ti_{0.91}O₃, BaTiO₃). Pyrolysis and adequate heat treatment were carried out in an air muffle furnace at 500 °C for 10 min for each spun-on coating. A final anneal in flowing O₂ at high temperature of 700 °C for 30 min. The compositionally graded thin film with Zr/Ti ratio varying from BaZr_{0.35}Ti_{0.65}O₃ at the substrate to BaTiO₃ at the top surface was formed in this study. The total thickness was about 680 nm.

The crystalline phase of the thin films was identified by X-ray diffraction (SIEMENS D-500 powder diffractometer). The film thickness and the surface morphology were determined by Field Emission Scanning Electron Microscope (FESEM). For electrical measurements the top gold electrode of a 200 μm square was deposited by DC-sputtering. Current–voltage (*I*–*V*) characteristics were measured using a HP 4140B. The capacitance–voltage (*C*–*V*) and capacitance–temperature (*C*–*T*) characteristics were measured using an Agilent 4284A LCR

meter. The sample's temperature was varied by using a delta chamber. Dielectric constant and dielectric loss of the films was measured at 100 kHz, with an AC field of 0.4 kV/cm superimposed on a slowly varying direct current (DC) bias field. The DC bias was stepped through 0.2 V intervals and held 1 s prior to capacitance measurement.

3. Results and discussion

Fig. 1 shows the XRD of the Ba(Zr_{0.35}Ti_{0.65}) thin films deposited on (a) LaNiO₃/Pt/Ti/SiO₂/Si and (b) Ba(Zr_{0.30}Ti_{0.70})/Pt/Ti/SiO₂/Si substrates, respectively, after annealing at 700 °C for 30 min. The perovskite phase for BZT thin films deposited on Pt/Ti/SiO₂/Si substrates had a preferred (1 1 0) orientation. Films deposited on LaNiO₃/Pt/Ti/SiO₂/Si substrates exhibited a highly (1 0 0) preferred orientation. No observable impurity phases were found. The LNO layer not only serves as a useful metal oxide bottom electrode, but also forms a template with preferred (1 0 0) orientation to enable growth of high quality BZT films. Pt-buffer substrate showed highly preferred (1 1 1) orientation (Fig. 1(b)) and enable growth of preferred (1 1 0) orientation BZT films. The XRD patterns revealed that the compositionally graded BaZr_xTi_{1–x}O₃ thin film was also (1 0 0) orientation structure and had a single perovskite phase, shown in Fig. 1(c). The degree of orientation of BZT thin films is shown as a function of seed layer thickness in Fig. 1 (inset figure). The relative intensity of the BZT (1 0 0) peak was calculated as $I_{(1\ 0\ 0)}(\%) = I_{(1\ 0\ 0)} / (I_{(1\ 0\ 0)} + I_{(1\ 1\ 0)})$. It is evidence that the relative intensity of (1 0 0) peaks was increased from 24% to 46% and then decreased to 20% with the increase of seed layer thickness. The (1 0 0) peak intensity of the BZT was obviously enhanced as the thickness of the seed layer increased up to 20 nm. However, as the seed layer thickness was further increased to 30 nm, the (1 0 0) orientation of BZT thin film was decreased. The full width at half-maximum (FWHM) of the (1 1 0) was decreased with the insertion of the seed layer. It can be attributed to the higher degree of crystal

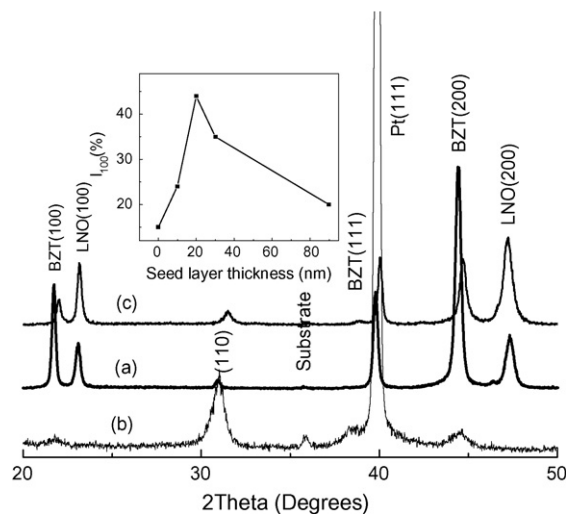


Fig. 1. XRD patterns of sol-gel deposited BaZr_{0.35}Ti_{0.65}O₃ thin films on (a) LaNiO₃/Pt/Ti/SiO₂/Si(1 0 0), (b) BaZr_{0.30}Ti_{0.70}O₃/Pt/Ti/SiO₂/Si(1 0 0) substrates and (c) BZT compositionally graded films.

with seed layer than unseeded ones. The thin seed layer of BZT will provide the nucleation sites to promote the nucleation and growth of BZT films.

Fig. 2 shows SEM images of the sol–gel deposited $\text{BaZr}_{0.35}\text{Ti}_{0.65}\text{O}_3$ thin films on (a) $\text{LaNiO}_3/\text{Pt}/\text{Ti}/\text{SiO}_2/\text{Si}(1\ 0\ 0)$ and (b) $\text{Pt}/\text{Ti}/\text{SiO}_2/\text{Si}$ substrates. As shown in Fig. 2, BZT thin films deposited on $\text{Pt}/\text{Ti}/\text{SiO}_2/\text{Si}$ substrate have the smaller grain size and denser structure than that of the thin film deposited on $\text{LNO}/\text{Pt}/\text{Ti}/\text{SiO}_2/\text{Si}$ substrate. The morphologies of thin film deposited on $\text{LNO}/\text{Pt}/\text{Ti}/\text{SiO}_2/\text{Si}$ substrate show 30–40 nm grain size, and presumably the (1 0 0) preferred orientation LNO grains in the buffer layer could serve as seeds for the subsequently deposited crystalline BZT film. We also observed the SEM surface of BZT thin films deposited onto the $\text{Pt}/\text{Ti}/\text{SiO}_2/\text{Si}$ substrates and seed layers with difference thickness (not shown in this paper). The grain size and morphologies of the BZT thin films were not obviously affected by the existence of seed layers. The variation of grain size and grain morphologies was mainly controlled by the nucleation and growth rate, which were influenced by the annealing temperature, substrates and composition. It is envisaged that for sufficiently dilute spin-on solution, the single-coated layer is very thin (e.g. ~ 8.5 nm for 0.1 M concentration) and the condensation rate is low, therefore local grain-on-grain, or homoepitaxy, grown at the interface between the new coating layer and the former coated layer would occur, thus resulting in highly preferred orientation. The existence of a seed layer on the bottom of a sol–gel film with an equivalent crystallographic lattice, can be regarded as a preferential site over which the nucleation of the perovskite phase will easily take place.

Fig. 3 shows the room temperature dielectric constant vs. electric field behaviors. The loss tangent measurements as a function of bias voltage gave curves of similar shape to the tuning curves. Losses for all samples were less than 2% at room temperature and zero bias. The $\text{BaZr}_{0.35}\text{Ti}_{0.65}\text{O}_3$ thin films derived on $\text{LaNiO}_3/\text{Pt}/\text{Ti}/\text{SiO}_2/\text{Si}$ substrates had larger dielectric constant and higher leakage current than that of thin film prepared on $\text{Pt}/\text{Ti}/\text{SiO}_2/\text{Si}$ substrates. The leakage current of thin film prepared on $\text{Pt}/\text{Ti}/\text{SiO}_2/\text{Si}$ substrates and $\text{LaNiO}_3/\text{Pt}/\text{Ti}/\text{SiO}_2/\text{Si}$ substrates was 3.8×10^{-5} A/cm² and 1.27×10^{-4} A/cm², respectively, at an applied electric field of

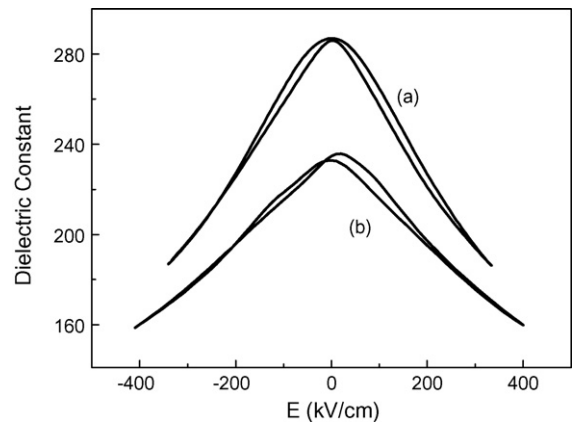


Fig. 3. ϵ – E characteristics of $\text{BaZr}_{0.35}\text{Ti}_{0.65}\text{O}_3$ thin films on (a) $\text{LaNiO}_3/\text{Pt}/\text{Ti}/\text{SiO}_2/\text{Si}(1\ 0\ 0)$ and (b) $\text{Pt}/\text{Ti}/\text{SiO}_2/\text{Si}(1\ 0\ 0)$ substrates (measurement frequency 100 kHz).

200 kV/cm. A possible explanation for these different electric properties could be due to the influence of the grain structure [16], orientation and strain [17]. Presumably the highly oriented grains in the LNO buffer layer could serve as a template for the subsequently deposited crystalline BZT thin film with high orientation and larger grain sizes. The films with larger grain sizes and more aligned grain configurations have overall shorter conduction paths along the grain boundaries, which causes an increase in the leakage current. This result is in agreement with the SEM images.

Experimental results showed that LNO as bottom electrode lead to an enhancement in (1 0 0)-orientation, and they had larger dielectric constant, dielectric loss and leakage current than that of Pt bottom electrode, in agreement with the analysis of XRD and SEM images. In order to optimize the dielectric properties of BZT thin films prepared on $\text{Pt}/\text{Ti}/\text{SiO}_2/\text{Si}$ substrates which has low dielectric loss and leakage current, we choose the $\text{Ba}(\text{Zr}_{0.30}\text{Ti}_{0.70})$ as seed layer to analyze the relationship of seed layer, microstructure and dielectric behavior of the thin films. Figs. 4 and 5 show the relationship between dielectric constant, dielectric loss and tunability as a function of seed layer thickness. The dielectric loss of BZT thin films decreased with increasing in thickness of seed layer. The tunability and dielectric constant of BZT

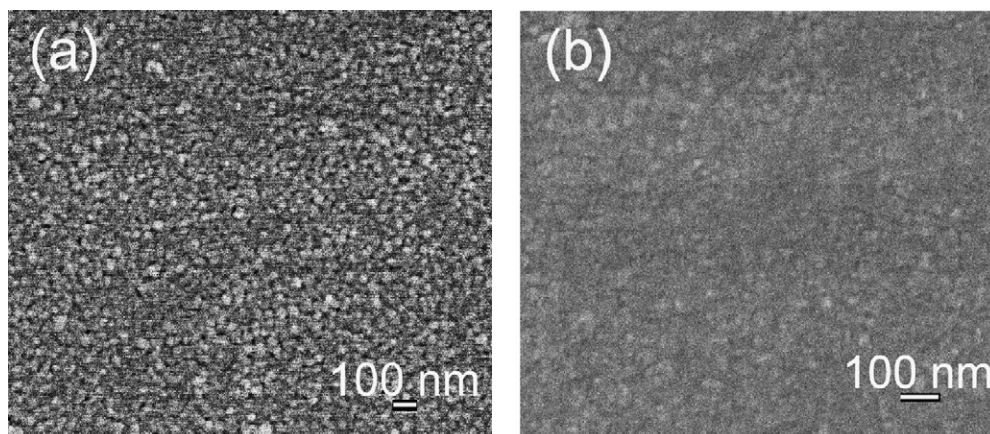


Fig. 2. SEM micrographs of sol–gel deposited $\text{BaZr}_{0.35}\text{Ti}_{0.65}\text{O}_3$ thin films on (a) $\text{LaNiO}_3/\text{Pt}/\text{Ti}/\text{SiO}_2/\text{Si}$ and (b) $\text{Pt}/\text{Ti}/\text{SiO}_2/\text{Si}$ substrates.

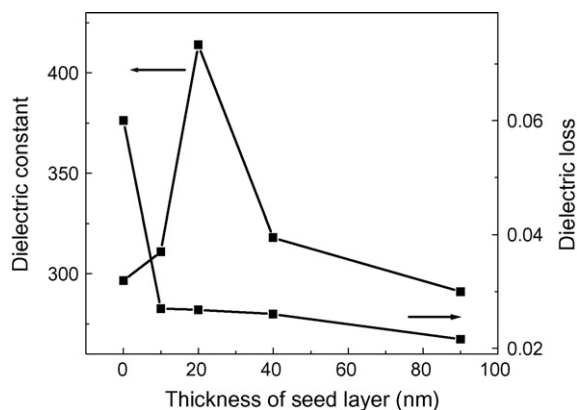


Fig. 4. The dielectric constant and dielectric loss of $\text{BaZr}_{0.30}\text{Ti}_{0.35}\text{O}_3$ thin films as a function of $\text{BaZr}_{30}\text{Ti}_{70}\text{O}_3$ seed layer thickness (frequency 100 kHz).

films showed a maximum value of 37% and 410, respectively, at a seed layer thickness of 20 nm. Meanwhile, the leakage current was decreased from $1.1 \times 10^{-6} \text{ A/cm}^2$ to $8.7 \times 10^{-8} \text{ A/cm}^2$ at an applied electric field of 250 kV/cm, shown in Fig. 6. The leakage current reached a minimum and the dielectric constant and tunability reached a maximum for BZT thin films with 20 nm seed layer. These results are similar to the case previously reported by Lee et al. [4,18]. The XRD results revealed that the effect of the seed layers on the orientation and microstructure of BZT films is dependent on the thickness of the seed layer, with an optimal thickness existing for the maximization of the degree of orientation and, consequently, of the dielectric and tunability properties. This improved dielectric constant and tunability when inserting seed layers are partly attributed to the increase of the grain size and to the (1 0 0) preferred orientation of the film leading to an enhancement of the in-plane oriented polar axis. On the other hand, it was also suggested that the seed layer insertion would result in the suppression of the formation of a low dielectric constant interfacial layer between the film and the electrode, ending in improved dielectric properties [4].

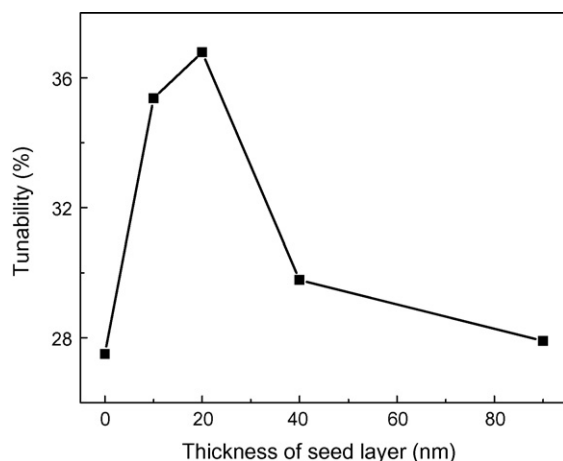


Fig. 5. Tunability of $\text{BaZr}_{0.30}\text{Ti}_{0.35}\text{O}_3$ thin films as a function of $\text{BaZr}_{30}\text{Ti}_{70}\text{O}_3$ seed layer thickness (electric field 200 kV/cm, frequency 100 kHz).

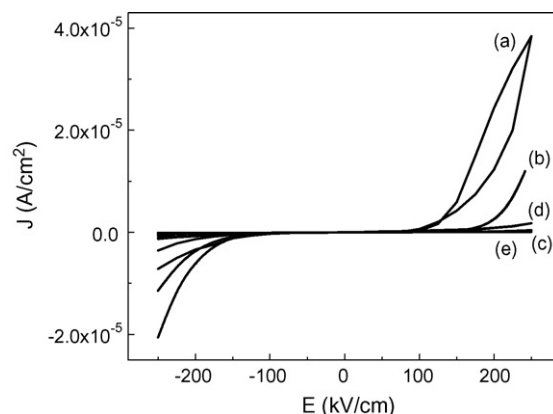


Fig. 6. J - E curves of $\text{BaZr}_{0.30}\text{Ti}_{0.35}\text{O}_3$ thin films for different seed layer thickness (a) 0 nm, (b) 10 nm, (c) 20 nm, (d) 40 nm and (e) 90 nm.

It was reported that the tunability and dielectric constant of 160 nm thick BST films deposited by PLD technology showed a maximum of 53% and 720, respectively at a seed layer thickness of 10 nm. An improvement in dielectric properties was achieved by the insertion of seed layers at the BZT/Pt interface by sol-gel processing. The strain due to the lattice mismatch, a dead layer near the interface, and local polar regions near the charged defects like oxygen vacancy are expected to affect the dielectric properties of the thin films. Among them, the strain in the films is one of the most critical problems, since the low frequency dielectric properties are closely related to the ionic motions in crystal structures [19]. The differences in dielectric constant, dielectric loss and tunability with various seed thickness were obtained, probably as a result of the existence of anisotropic in-plane strain and the grain morphologies within the BZT films [20]. The anisotropic in-plane strain among the individual layers was resulted from the different thickness and annealing time of seed layer. The optimized seed layer thickness for BZT deposition onto Pt/Ti/SiO₂/Si substrates plays an important role in maintaining the high tunability and low dielectric loss, which are suitable for microwave device applications.

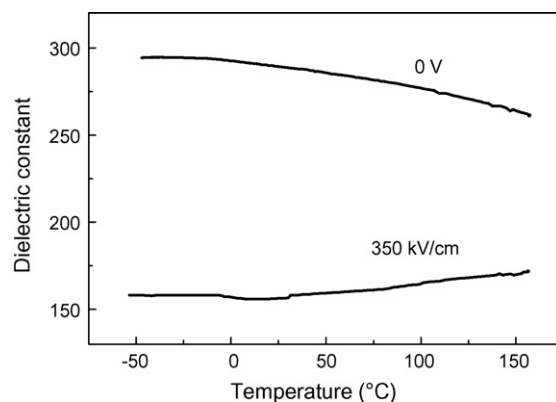


Fig. 7. Temperature dependence of the dielectric constant at 0 kV/cm and 350 kV/cm electric fields for BZT compositionally graded thin films, respectively (measurement frequency 1 MHz).

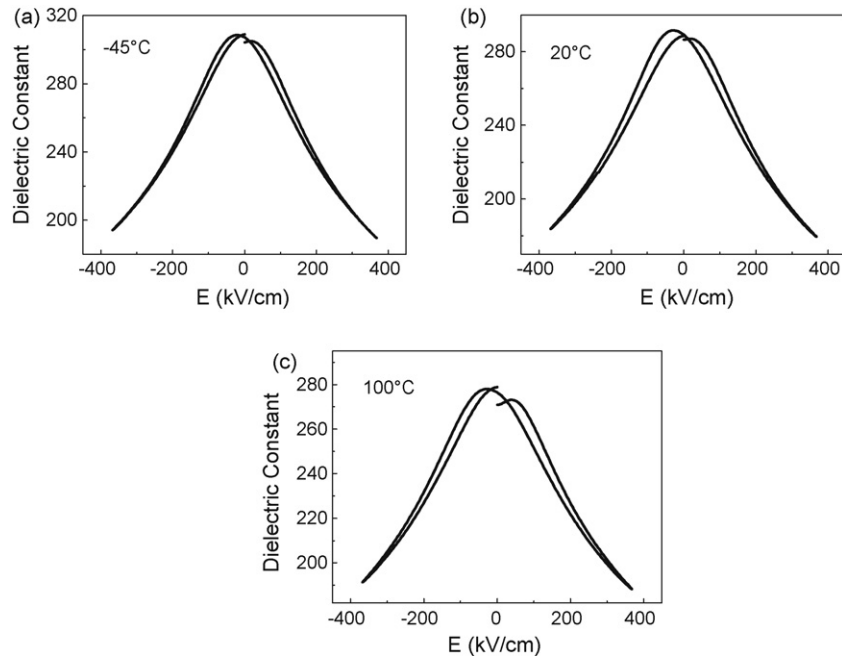


Fig. 8. ϵ - E characteristics of BZT compositionally graded thin films measured at (a) -45°C , (b) 20°C and (c) 100°C (measurement frequency 1 MHz).

Fig. 7 showed the temperature dependence of dielectric constant as a function of externally applied DC voltage for the compositionally graded thin films, all measured at 1 MHz frequency. In $\text{Ba}(\text{Zr}_x\text{Ti}_{1-x})\text{O}_3$, the Curie temperature, T_c , can be controlled by varying the mole fraction x of Zr. It is evident that the phase transition of $\text{Ba}(\text{Zr}_x\text{Ti}_{1-x})\text{O}_3$ thin films with (a) $x = 0$, (b) $x = 0.05$, (c) $x = 0.16$, and (d) $x = 0.35$ occurs at about 150°C , 52°C , -15°C , and -80°C , respectively [21]. Therefore, the composition-dependent Curie temperature should manifest itself in the compositionally graded BZT film to show a smeared or expanded diffuse transition. The graded thin films exhibited a diffused phase transition accompanied by a diffused peak in the temperature variations of dielectric constants. The data reveal a relatively flat profile, especially in the temperature range between -50°C and 120°C . The change of dielectric constant vs. DC bias field is quite appreciable, indicating a high tunability over a wide temperature range. The $\text{BaZr}_x\text{Ti}_{1-x}\text{O}_3$ compositionally graded thin films which the dielectric constant showed insensitive temperature dependence could be attributed to the presence of a distribution of phases (phase transition from ferroelectric to paraelectric) in the film.

Fig. 8 shows dielectric constant vs. electric field characteristics at different temperature. The loss tangent measurements as a function of bias voltage gave curves of similar shape to the tuning curves. Loss for sample was less than 2%. It was revealed that the compositionally graded BZT had high tunability in a wide temperature range. The tunability of compositionally graded thin films is about 46%, at an applied field of 400 kV/cm and measurement frequency of 1 MHz. The tunability of graded thin films is larger than that of homogeneous thin films. Generally, ferroelectric material is tunable in only a narrow temperature range near a phase

transition. Compositionally graded $\text{Ba}(\text{Zr}_x\text{Ti}_{1-x})\text{O}_3$ films with high tunability and weak temperature dependence of tunability in the temperature range between -50°C and 120°C could make attractive devices.

4. Conclusions

The XRD patterns revealed that the perovskite phase for BZT thin films deposited on Pt/Ti/SiO₂/Si substrates had a preferred (1 1 0) orientation and exhibited a highly (1 0 0) preferred orientation when the thin films were deposited on LaNiO₃/Pt/Ti/SiO₂/Si substrates. No impurity phases were observed. The dielectric loss of BZT thin films decreased with increasing of seed layer thickness. The leakage current reached a minimum and the dielectric constant and tunability reached a maximum for BZT thin films with 20 nm seed layer. It was indicated that the BZT thin film with 20 nm seed layer had better dielectric tunability properties. The change of dielectric constant vs. DC bias field is quite appreciable for the compositionally graded BZT thin film. No steep phase transition peak was observed in the temperature range from -50 to 120°C . Both dielectric constant and tunability showed weak temperature dependence.

Acknowledgements

This research was supported by the Ministry of Sciences and Technology of China through 973-project under Grant 2002CB613304, Shanghai Nano Fundamental Committee under Contract No. 05nm05028, Specialized Research Fund for the Doctoral Program of Higher Education (20060247003). The work described in this paper was partially supported by a Grant from CityU (Project No. 7001828).

References

- [1] E.A. Fardin, A.S. Holland, K. Ghorbani, P. Reichart, Enhanced tunability of magnetron sputtered $\text{Ba}_{0.5}\text{Sr}_{0.5}\text{TiO}_3$ thin films on *c*-plane sapphire substrates, *Appl. Phys. Lett.* 89 (2006) 022901.
- [2] K.B. Chong, L. Chen, L. Yan, C.Y. Tan, T. Yang, C.K. Ong, T. Osipowicz, Improvement of dielectric loss tangent of Al_2O_3 doped $\text{Ba}_{0.5}\text{Sr}_{0.5}\text{TiO}_3$ thin films for tunable microwave devices, *J. Appl. Phys.* 95 (2004) 1416–1419.
- [3] A.K. Tagantsev, V.O. Sherman, K.F. Astafiev, J. Venkatesh, N. Setter, Ferroelectric materials for microwave tunable applications, *J. Electroceram.* 11 (2003) 5–66.
- [4] Z. Fu, A.Y. Wu, M.V. Paula, Effect of seed layer thickness on texture and electrical properties of sol–gel derived $(\text{Ba}_{0.8}\text{Sr}_{0.2})\text{TiO}_3$ thin films, *Chem. Mater.* 18 (2006) 3343–3350.
- [5] T.B. Wu, C.M. Wu, M.L. Chen, Highly insulative barium zirconate–titanate thin films prepared by RF-magnetron sputtering for dynamic random access memory applications, *Appl. Phys. Lett.* 69 (1996) 2659–2661.
- [6] R. Farhi, M.E. Marssi, A. Simon, J. Ravez, A Raman and dielectric study of ferroelectric $\text{Ba}(\text{Ti}_{1-x}\text{Zr}_x)\text{O}_3$ ceramics, *Eur. Phys. J. B* 9 (1999) 599–604.
- [7] W.S. Choi, B.S. Jang, D.G. Lim, J.S. Yi, B.Y. Hong, Characterization of $\text{Ba}(\text{Zr}_{0.2}\text{Ti}_{0.8})\text{O}_3$ thin films deposited by RF-magnetron sputtering, *J. Cryst. Growth* 237–239 (2002) 438–442.
- [8] J.W. Zhai, X. Yao, L.Y. Zhang, B. Shen, Dielectric nonlinear characteristics of $\text{Ba}_{0.35}\text{Zr}_{0.65}\text{TiO}_3$ thin films grown by a sol–gel process, *Appl. Phys. Lett.* 84 (2004) 3136–3138.
- [9] J. Ravez, C. Broustera, A. Simon, Lead-free ferroelectric relaxor ceramics in the BaTiO_3 – BaZrO_3 – CaTiO_3 system, *J. Mater. Chem.* 9 (1999) 1609–1613.
- [10] Z. Yu, R. Guo, A.S. Bhalla, Growth of $\text{Ba}(\text{Ti}_{1-x}\text{Zr}_x)\text{TiO}_3$ single crystals by the laser heated pedestal growth technique, *J. Cryst. Growth* 233 (2001) 460–465.
- [11] F. Zimmermann, M. Voigts, W. Menesklou, E. Ivers-Tiffée, $\text{Ba}_{0.6}\text{Sr}_{0.4}\text{TiO}_3$ and $\text{BaZr}_{0.3}\text{Ti}_{0.7}\text{O}_3$ thick films as tunable microwave dielectrics, *J. Eur. Ceram. Soc.* 24 (2004) 1729–1733.
- [12] S. Halder, U. Bottger, R. Waser, Fabrication and electrical characterization of Zr-substituted BaTiO_3 thin films, *Appl. Phys. A* 81 (2004) 25–29.
- [13] J. Xu, W. Menesklou, E. Ivers-tiffée, Annealing effects on structural and dielectric properties of tunable BZT thin films, *J. Electroceram.* 13 (2004) 229–233.
- [14] J.W. Zhai, D. Hu, X. Yao, Z.K. Xu, H.D. Chen, Preparation and tunability properties of $\text{Ba}(\text{Zr}_x\text{Ti}_{1-x})\text{O}_3$ thin films grown by a sol–gel process, *J. Eur. Ceram. Soc.* 26 (2006) 1917–1920.
- [15] H.Y. Lee, T.B. Wu, Crystallization kinetics of sputter-deposited LaNiO_3 thin films on Si substrate, *J. Mater. Res.* 13 (1998) 2291–2294.
- [16] C.B. Parker, J.P. Maria, A.I. Kingon, Temperature and thickness dependent permittivity of $(\text{Ba}, \text{Sr})\text{TiO}_3$ thin films, *Appl. Phys. Lett.* 81 (2002) 340–342.
- [17] S. Bhaskar, S.B. Majumder, R.S. Katiyar, Diffuse phase transition and relaxor behavior in $(\text{PbLa})\text{TiO}_3$ thin films, *Appl. Phys. Lett.* 80 (2002) 3997–3999.
- [18] Y.A. Jeon, W.C. Shin, T.S. Seo, S.G. Yoon, Improvement in tunability and dielectric loss of $(\text{Ba}_{0.5}\text{Sr}_{0.5})\text{TiO}_3$ capacitors using seed layers on $\text{Pt}/\text{Ti}/\text{SiO}_2/\text{Si}$ substrates, *J. Mater. Res.* 17 (2002) 2831–2836.
- [19] S. Hyun, K. Char, Effects of strain on the dielectric properties of tunable dielectric SrTiO_3 thin films, *Appl. Phys. Lett.* 79 (2001) 254–256.
- [20] C.M. Carlson, T.V. Rivkin, P.A. Parilla, J.D. Perkins, D.S. Ginley, Large dielectric constant $\text{Ba}_{0.4}\text{Sr}_{0.6}\text{TiO}_3$ thin films for high-performance microwave phase shifters, *Appl. Phys. Lett.* 76 (2000) 1920–1922.
- [21] J.W. Zhai, X. Yao, J. Shen, L.Y. Zhang, H.D. Chen, Structural and dielectric properties of $\text{Ba}(\text{Zr}_x\text{Ti}_{1-x})\text{O}_3$ thin films prepared by the sol–gel process, *J. Phys. D: Appl. Phys.* 37 (2004) 748–752.